International Journal of Cardiology 296 (2019) 129–135

Contents lists available at ScienceDirect

International Journal of Cardiology

journal homepage: www.elsevier.com/locate/ijcard

Loss of Rubicon ameliorates doxorubicin-induced cardiotoxicity through enhancement of mitochondrial quality

Xiaoyun Liu [a, b], Shasha Zhang [a, b], Lin An [a, b], Jian Wu [c], Xiaowen Hu [a, b], Shuaiwei Lai [a, b], Haniya Mazhar [a, b], Yunzeng Zou [c], Lin He [a, b], Hongxin Zhu [a, b, *]

[a] Bio-X-Renji Hospital Research Center, Renji Hospital, School of Medicine, Shanghai Jiao Tong University, Shanghai, China
[b] Bio-X Institutes, Key Laboratory for the Genetics of Developmental and Neuropsychiatric Disorders, Ministry of Education, Shanghai Jiao Tong University, Shanghai, China
[c] Shanghai Institute of Cardiovascular Diseases, Zhongshan Hospital and Institutes of Biomedical Sciences, Fudan University, Shanghai, China

ARTICLE INFO

Article history:
Received 20 February 2019
Received in revised form
5 July 2019
Accepted 23 July 2019
Available online 24 July 2019

Keywords:
Rubicon
Doxorubicin
Cardiotoxicity
Autophagy
Mitophagy
Mitochondrial dynamics

ABSTRACT

Background: The therapeutic potential of doxorubicin (DOX) is limited by cardiotoxicity. Rubicon is an inhibitory interacting partner of autophagy protein UVRAG. Currently, the role of Rubicon in DOX-induced cardiotoxicity is unknown. In this study, we test the hypothesis that loss of Rubicon attenuates DOX-induced cardiotoxicity.
Methods: A mouse model of acute DOX-induced cardiotoxicity was established by a single intraperitoneal injection of DOX at a dose of 20 mg/kg. Rubicon expression was detected by Western blot. Cardiac damage was determined by measuring activities of lactate dehydrogenase and myocardial muscle creatine kinase in the serum, cytoplasmic vacuolization, collagen deposition, ROS levels, ATP content and mitochondrial damage in the heart. Cardiac morphometry and function were assessed by echocardiography. Markers for autophagy, mitophagy and mitochondrial dynamics were evaluated by Western blot and real time reverse transcription polymerase chain reaction.
Results: Rubicon expression was reduced in the heart 16 h after DOX treatment. DOX induced accumulation of cytoplasmic vacuolization and collagen, increased serum activities of lactate dehydrogenase and myocardial muscle creatine kinase, enhanced ROS levels, reduced ATP content, pronounced mitochondrial damage and greater left ventricular wall thickness in wild type mice, which were mitigated by Rubicon deficiency. Mechanistically, loss of Rubicon improved DOX-induced impairment of autophagic flux, Parkin-mediated mitophagy and mitochondrial fission and fusion in the heart.
Conclusions: Loss of Rubicon ameliorates DOX-induced cardiotoxicity through enhancement of mitochondrial quality by improving autophagic flux, mitophagy and mitochondrial dynamics. Rubicon is a potential molecular target for prevention and therapy of DOX cardiotoxicity.

1. Introduction

Doxorubicin (DOX) is one of the most potent chemotherapy agents. However, its clinical use is limited by potential development of cardiotoxicity. Oxidative stress caused by increased reactive oxygen species (ROS) has been considered as one of the major mediators of DOX cardiotoxicity [1–3]. As an electron acceptor, DOX induces mitochondrial ROS generation. Increased ROS causes mitochondrial damage, which in turn, amplifies ROS production, forming a vicious cycle. This ROS-induced ROS release ultimately leads to cardiac damage and heart failure [4]. Therefore, DOX cardiotoxicity may be ameliorated through enhancement of mitochondrial quality, which is mainly governed by mitophagy and mitochondrial dynamics [5].

Macroautophagy (hereafter referred to as autophagy) is an evolutionally conserved pathway delivering cytoplasmic contents to lysosome for degradation [6]. Mitophagy is a type of autophagy that selectively removes damaged mitochondria. Mitophagy occurs under baseline conditions and stress conditions such as oxidative stress to maintain cellular functions [7]. Mitophagy is regulated by PTEN-induced kinase 1 (PINK1) and Parkin proteins [8,9]. PINK1 controls Parkin translocation from cytoplasm to mitochondria [10]. Mitochondrial Parkin ubiquitinates target proteins localized on the outer mitochondrial membrane, which mediate mitochondrial degradation by autophagy [11]. Animals deficient for Parkin show reduced

* Corresponding author at: Bio-X-Renji Hospital Research Center, Renji Hospital, School of Medicine, Shanghai Jiao Tong University, Shanghai, China, Bio-X Institutes, Key Laboratory for the Genetics of Developmental and Neuropsychiatric Disorders, Ministry of Education, Shanghai Jiao Tong University, Shanghai, China.
E-mail address: hxzhu@sjtu.edu.cn (H. Zhu).

https://doi.org/10.1016/j.ijcard.2019.07.074
0167-5273/

mitophagy and accumulation of damaged mitochondria, leading to cardiac dysfunction under physiological and stress conditions [12,13].

Mitochondrial dynamics including mitochondrial fusion and fission are also critical for mitochondrial quality control [14]. Mitochondrial fusion is regulated by Mitofusin1 (MFN1), Mitofusin2 (MFN2), and optic atrophy factor 1 (OPA1) proteins [14]. Mitochondrial fission is mainly regulated by a large GTPase dynamin-related protein 1 (Drp1) [15]. A number of proteins including mitochondrial fission 1 protein (Fis1), mitochondrial fission factor (Mff), mitochondrial division factors 49 and 51 kDa proteins (Mid49 and Mid51) interact with Drp1. For mitochondrial fission, these proteins coordinate to recruit Drp1 from cytoplasm to mitochondria [15]. Under physiological conditions, mitochondrial fusion and fission are delicately balanced. Disturbance in the balance between mitochondrial fusion and fission causes heart disease [15–17].

Ultraviolet irradiation resistance-associated gene (UVRAG), an autophagy-related gene, regulates autophagosome maturation [18,19]. Rubicon (Run domain Beclin-1-interacting and cysteine-rich domain-containing protein) binds to UVRAG and inhibits UVRAG-mediated autophagosome maturation [20,21]. Previously we and others have shown that DOX disrupts multiple steps of autophagy in the heart including autophagosome formation, maturation and degradation [22–25]. It remains unknown whether Rubicon plays a role in autophagy impairment in DOX cardiotoxicity. In this study, we test the hypothesis that loss of Rubicon ameliorates DOX-induced DOX cardiotoxicity through improving autophagy and mitochondrial quality.

2. Materials and methods

2.1. Animal experiments

All mice used were on the FVB/NJ background. Animal protocols were approved by the Institutional Animal Care and Use Committee of Shanghai, China [SYXK (SH) 2011-0112]. Seven-week-old male mice were used for experiments unless stated otherwise. Generation of Rubicon-deficient mice was described previously [26,27]. A single dose of DOX (BBI, Canada) at 20 mg/kg was injected intraperitoneally into mice to establish acute DOX cardiotoxicity. For assessment of cardiac morphometry and function, mice were intraperitoneally injected with DOX (4 mg/kg) weekly for 4 weeks and then subjected to echocardiography.

2.2. Antibodies

Rabbit anti-LC3 polyclonal antibody was from MBL International Corporation. Rabbit anti-Rubicon monoclonal antibody, rabbit anti-UVRAG polyclonal antibody, rabbit anti-LC3 polyclonal antibody, rabbit anti-p62 polyclonal antibody and rabbit anti-VDAC polyclonal antibody were purchased from Cell Signaling Technology. Mouse anti-Parkin monoclonal antibody, rabbit anti-GAPDH polyclonal antibody, mouse anti-Fis1 monoclonal antibody, mouse anti-Drp1 monoclonal antibody and mouse anti-Opa1 monoclonal antibody were purchased from Santa Cruz Biotechnology. Mouse anti-α-tubulin monoclonal antibody was obtained from Proteintech Group, Inc.

2.3. Western blot

Proteins were separated by SDS-PAGE electrophoresis and transferred to nitrocellulose membrane. The membrane was blocked for 1 h at room temperature. Then the membrane was incubated with primary antibodies overnight at 4 °C and probed with HRP-coupled secondary antibodies for 1 h at room temperature. The protein chemiluminescent signals were imaged using Immobilon™ Western Chemiluminescent HRP Substrate (Millipore).

2.4. Histology

Mice were deeply anesthetized and the hearts were perfused with phosphate buffered saline (PBS), which was followed by fixation by 4% paraformaldehyde. The hearts were then embedded in paraffin and serial sections of 5 μm were cut (Leica RM2255). H&E staining was performed to evaluate cardiac morphology and Picrosirius red staining was conducted to assess collagen deposition.

2.5. Measurement of serum activities of lactate dehydrogenase (LDH) and myocardial muscle creatine kinase (CK-MB)

Serum activities of LDH and CK-MB were examined using LDH detection kit (Nanjing Jiancheng Bioengineering Institute, Nanjing, China) and CK-MB ELISA kit (Nanjing Jiancheng Bioengineering Institute, Nanjing, China), respectively. The assays were carried out according to the manufacturer's instructions.

2.6. ATP measurement

ATP content in myocardial tissues was determined using ATP assay kit (Nanjing Jiancheng Bioengineering Institute, Nanjing, China) according to the manufacturer's protocol.

2.7. ROS measurement

ROS analysis was performed as described previously [22]. In brief, fresh heart tissues were homogenized in 40 mM Tris–HCl buffer (pH 7.4) on ice. The homogenates were then diluted to 0.25% with the identical buffer and incubated with 1.25 mM 2′,7′-dichlorofluorescin-diacetate (DCFH-DA, Sigma-Aldrich) at 37 °C for 30 min. The intensity of fluorescence was detected with excitation wavelength at 488 nm and emission wavelength at 535 nm.

2.8. Electron microscopy

Mouse hearts were dissected and left ventricles were cut into small pieces (<1 mm^3), which were fixed with 2.5% glutaraldehyde in 0.1 M phosphate buffer (pH 7.4) at 4 °C for 2 h. The samples were then postfixed with 1% osmium tetroxide and routinely processed for transmission electron microscopic observation.

2.9. Autophagic flux assessment

In vivo autophagic flux assessment was conducted as described previously [22]. In brief, mice were intraperitoneally injected with vehicle (ddH_2O) or chloroquine (CQ, 50 mg/kg, Sigma-Aldrich) and left ventricles were dissected 6 h after injection. Then proteins were extracted and Western blot was performed to evaluate protein levels of LC3 II and p62.

2.10. Isolation of cardiac mitochondria

Left ventricles dissected from the mice were homogenized in MSE buffer (Mannitol 220 mM, Sucrose 70 mM, MOPS 5 mM, EGTA 2 mM, BSA 0.2%) for 2–3 s. Tissue homogenates were centrifuged at 200g at 4 °C for 5 min and the supernatant was collected. The supernatant was centrifuged at 8500g at 4 °C for 10 min. The resulting supernatant (cytoplasmic fraction) was transferred into a new centrifuge tube and he pellet (mitochondrial fraction) was washed twice using MSE buffer. The final mitochondrial pellet was resuspended in the buffer containing 220 mM Mannitol, 70 mM Sucrose, 5 mM MOPS, 0.5 mM EGTA and 0.2% BSA.

2.11. Real-time reverse transcription polymerase chain reaction

Total RNA was extracted from left ventricles using TRIzol® and cDNA was synthesized using PrimeScript™ RT reagent Kit with gDNA Eraser for RT-PCR (TaKaRa). Gene expression was analyzed using FastStart Universal SYBR Green Master (Rox) system (Roche). *Gapdh* was used as internal control. Real-time reverse transcription polymerase chain reaction (RT-PCR) was carried out in triplicate for each cDNA sample. The primers for real-time RT-PCR were listed in Supplementary Table S1.

2.12. Echocardiography

Echocardiography was performed as described previously [27]. Briefly, mice were anesthetized by inhaled isoflurane. Echocardiographic imaging was performed using a Vevo 770 platform (VisualSonics, Canada) equipped with a 45 MHz imaging transducer. M-mode imaging was used to determine left ventricular contractility, cavity dimension and wall thickness. Measurements were carried out at least in triplicate.

2.13. Statistical analysis

All values were expressed as mean ± SEM. The Student's *t*-test was used for the comparison between two means and two-way ANOVA followed by Bonferroni's post hoc test was used to compare the means of multiple groups. Values of $P < 0.05$ were considered statistically significant.

3. Results

3.1. Rubicon expression in the heart after DOX treatment

We first assessed Rubicon expression in the hearts from DOX-treated wild type (WT) mice. Rubicon protein levels were significantly reduced 16 h after DOX treatment (Fig. 1A and B). However, Rubicon protein levels remained unaltered 3 and 5 days after DOX treatment (Fig. 1A and B). The absence of Rubicon protein in the hearts from Rubicon-deficient mice was confirmed by Western blot (Fig. 1C).

3.2. Loss of Rubicon improves survival in DOX-treated animals

WT mice began to die 4 days after DOX treatment (Fig. 1D). All male and female WT mice died 8 and 6 days after DOX treatment, respectively (Fig. 1D). However, approximately 20% male and 30%

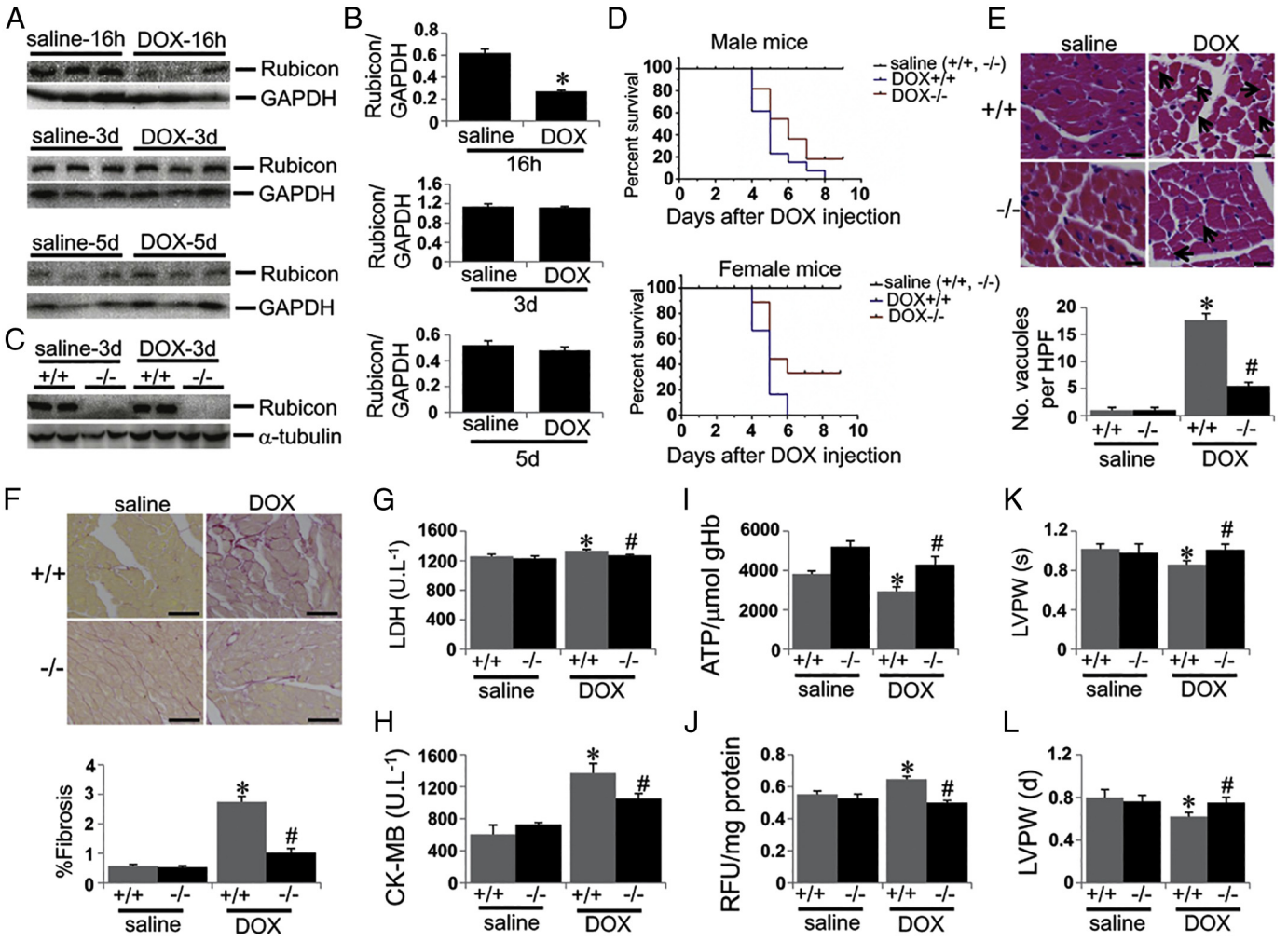

Fig. 1. Loss of Rubicon ameliorates DOX-induced cardiotoxicity. (A) Representative images of Rubicon expression in the hearts from DOX-treated WT mice. (B) Quantification of Rubicon as illustrated in (A) (n = 6). (C) Absence of Rubicon in the hearts from Rubicon-deficient mice was confirmed by Western blot. (D) Kaplan-Meier survival curves of DOX-treated mice. (For male mice, n = 10 for saline+/+, n = 9 for saline−/−, n = 9 for DOX+/+, n = 8 for DOX−/−. For female mice, n = 10 for saline+/+, n = 8 for saline−/−, n = 16 for DOX+/+, n = 13 for DOX−/−). (E) Photomicrographs of H&E-stained heart section. n = 3. Scale bars, 40 μm. Arrows indicate degenerative vacuoles. (F) Photomicrographs of Picrosirius red staining of cardiac section. n = 3. Scale bars, 80 μm. (G) Serum LDH activity in mice 3 days after DOX or saline treatment (n = 6–10). (H) Serum CK-MB activity in mice 3 days after DOX or saline treatment (n = 5–8). (I) ATP content in myocardial tissues from mice 3 days after DOX or saline treatment (n = 6–7). (J) ROS levels detected using DCFH-DA in the hearts from mice 3 days after DOX or saline treatment (n = 6). Systolic LVPW (K) and diastolic LVPW (L) evaluated by echocardiography. n = 6–9. $^{*}P < 0.05$ vs. saline+/+, $^{\#}P < 0.05$ vs. DOX+/+.

female Rubicon-deficient mice survived 9 days after DOX treatment (Fig. 1D), suggesting that loss of Rubicon improved survival in DOX-treated animals.

3.3. Loss of Rubicon ameliorates DOX-induced cardiotoxicity

We then investigated the effects of Rubicon deficiency on DOX-induced cardiac damage. Left ventricular cavity, which was enlarged in WT mice, appeared normal in Rubicon-deficient mice 3 days after DOX treatment (Supplementary Fig. S1). Cytoplasmic vacuolization, which was significantly increased in DOX-treated WT mice, was markedly decreased in DOX-treated Rubicon-deficient mice (Fig. 1E). In addition, collagen deposition was significantly reduced in Rubicon-deficient mice compared with WT controls after DOX treatment (Fig. 1F). The elevated serum activities of LDH and CK-MB in WT mice were attenuated by Rubicon deficiency after DOX treatment (Fig. 1G and H). Moreover, loss of Rubicon attenuated DOX-induced reduction in myocardial ATP content (Fig. 1I) and increase in ROS levels (Fig. 1J). Thus, loss of Rubicon mitigates DOX-induced cardiac damage. We then evaluated cardiac morphometry and function by echocardiography. To determine the potential clinical relevance of Rubicon-deficient mice, we treated the mice with a single dose of DOX (4 mg/kg) weekly for 4 weeks and then echocardiographic assessment was performed. Cardiac function in WT and Rubicon-deficient mice was not depressed after DOX treatment as evidenced by unaltered ejection fraction (EF) and fractional shortening (%FS) (Supplementary Fig. S2, Supplementary Table S2). However, systolic and diastolic left ventricular posterior wall (LVPW) thickness was significantly reduced in DOX-treated WT mice (Fig. 1K and L, Supplementary Fig. S2, Supplementary Table S2). Importantly, the reduction in LVPW was attenuated in Rubicon-deficient mice (Fig. 1K and L, Supplementary Fig. S2, Supplementary Table S2). The detailed echocardiographic data were presented in Supplementary Table S2. Combined, these data suggest that loss of Rubicon ameliorates DOX induced cardiotoxicity.

3.4. Mitochondrial damage is alleviated in the hearts from Rubicon-deficient mice after DOX treatment

The observation that increased ROS, the major cause of oxidative stress [3,28–30], was reduced and ATP content [31] was increased in the hearts from DOX-treated Rubicon-deficient mice suggest that

loss of Rubicon improves mitochondrial quality. We therefore examined mitochondrial structure in the heart using transmission electron microscopy. WT and Rubicon-deficient mice treated with saline exhibited normal mitochondrial structure (Fig. 2A and B). After DOX treatment, a substantial portion of mitochondria in WT mice showed sparse, shortened or broken cristae (Fig. 2C and D). Moreover, mitochondrial swelling occurred and mitochondria were even completely collapsed (Fig. 2D). However, mild mitochondrial damage was detected in DOX-treated Rubicon-deficient mice (Fig. 2E and F). These results demonstrate that loss of Rubicon alleviates DOX-induced mitochondrial damage in the heart.

3.5. Autophagic flux and mitophagy are improved in the hearts from Rubicon-deficient mice after DOX treatment

Damaged mitochondria are mainly cleared by mitophagy. Previously we have shown that DOX treatment impairs autophagic flux in the heart [22]. Thus, we first determined if loss of Rubicon improves DOX-induced impairment of autophagic flux. LC3 II and p62, two molecular markers for autophagy [32], were remarkably increased in DOX-treated WT mice (Fig. 3A–C), consistent with previous observation that DOX impairs autophagic degradation in the heart [22]. The increase in LC3 II and p62 was attenuated by Rubicon deficiency (Fig. 3A–C), suggesting that autophagic flux was improved. To confirm improved autophagic flux in DOX-treated Rubicon-deficient mice, we treated the mice with DOX alone or DOX in combination with CQ. In WT mice, LC3 II and p62 protein abundance were not significantly increased by combination treatment with DOX and CQ compared with DOX alone (Fig. 3E–G). However, in Rubicon-deficient mice, LC3 II and p62 protein abundance were significantly increased by combination treatment with DOX and CQ compared with DOX alone (Fig. 3E–G). Thus, loss of Rubicon improved autophagic flux in the hearts after DOX treatment. Protein levels of Rubicon interacting protein UVRAG were

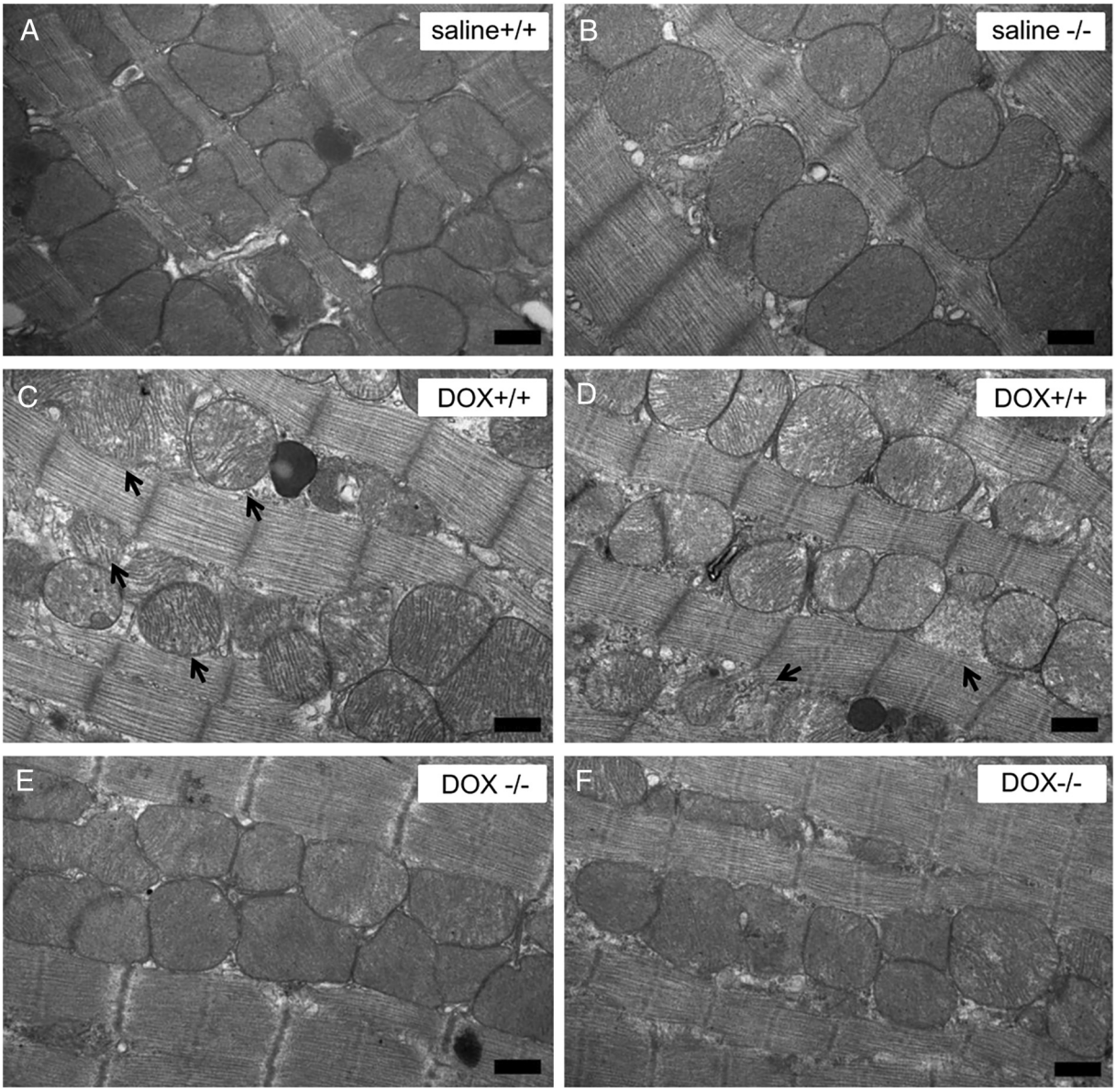

Fig. 2. Loss of Rubicon alleviates DOX-induced mitochondrial damage in the heart. Representative EM images for structural analysis of mitochondria in the hearts from WT and Rubicon-deficient mice 3 days after DOX or saline treatment. (A) WT mice treated with saline (saline+/+). (B) Rubicon-deficient mice treated with saline (saline−/−). (C, D) WT mice treated with DOX (DOX+/+). (E, F) Rubicon-deficient mice treated with DOX (DOX−/−) (scale bars, 500 nm). Arrows in (C) indicate damaged mitochondria with shortened, sparse or broken cristae. Arrows in (D) indicate collapsed mitochondria.

comparable between WT and Rubicon-deficient mice (Fig. 3A and D).

We then assessed Parkin-mediated mitophagy in the heart. Parkin protein levels were significantly reduced in the hearts from WT mice 3 days after DOX treatment (Fig. 3H and I); however, the reduction in Parkin protein was attenuated by Rubicon deficiency (Fig. 3H and I). To determine whether loss of Rubicon affected Parkin protein levels in mitochondria, we isolated mitochondria (Supplementary Fig. S3) and detected Parkin protein. After DOX treatment, Parkin protein levels in the mitochondria were significantly increased in Rubicon-deficient mice compared with WT controls (Fig. 3J and K). Conversely, Parkin protein levels in the cytoplasm were significantly reduced in Rubicon-deficient mice compared with WT controls after DOX treatment (Fig. 3L and M). Thus, disruption of Parkin expression and mitochondrial recruitment of Parkin were improved by Rubicon deficiency. VDAC, a mitochondrial marker, remained unaltered in DOX-treated animals (Supplementary Fig. S4). These data provide evidences suggesting that loss of Rubicon improves Parkin-mediated mitophagy after DOX treatment.

3.6. Loss of Rubicon regulates expression of markers for mitochondrial dynamics

Mitochondrial dynamics including mitochondrial fusion and fission also play prominent roles in mitochondrial quality control. To determine whether loss of Rubicon has impact on mitochondrial dynamics in the hearts after DOX treatment, we first examined expression of genes regulating mitochondrial fusion. *Opa1* mRNA levels were significantly reduced in WT mice after DOX treatment. The reduction in *Opa1* was blunted by Rubicon deficiency (Fig. 4A). Changes in *Opa1* expression was confirmed at protein levels (Fig. 4F and H). *Mfn1* and *Mfn2* expression was not changed in WT and Rubicon-deficient mice after DOX treatment (Fig. 4B and C). We then examined expression of genes regulating mitochondrial fission in the heart. *Fis1* mRNA expression was significantly decreased in DOX-treated WT mice and the decrease was attenuated by Rubicon deficiency (Fig. 4D). Alterations in *Fis1* expression induced by DOX were confirmed at protein levels (Fig. 4F and G). *Drp1* expression was comparable between DOX-treated WT and Rubicon-deficient mice (Fig. 4E, F and I). These results suggest that loss of Rubicon prevents DOX-induced dysregulation of markers for mitochondrial dynamics.

4. Discussion

The major findings of the present study are (i) loss of Rubicon ameliorates DOX-induced cardiotoxicity; (ii) DOX-induced mitochondrial damage in the heart is attenuated by Rubicon deficiency; and (iii) loss of Rubicon mitigates DOX-induced impairment of autophagic flux, mitophagy and mitochondrial dynamics in the heart.

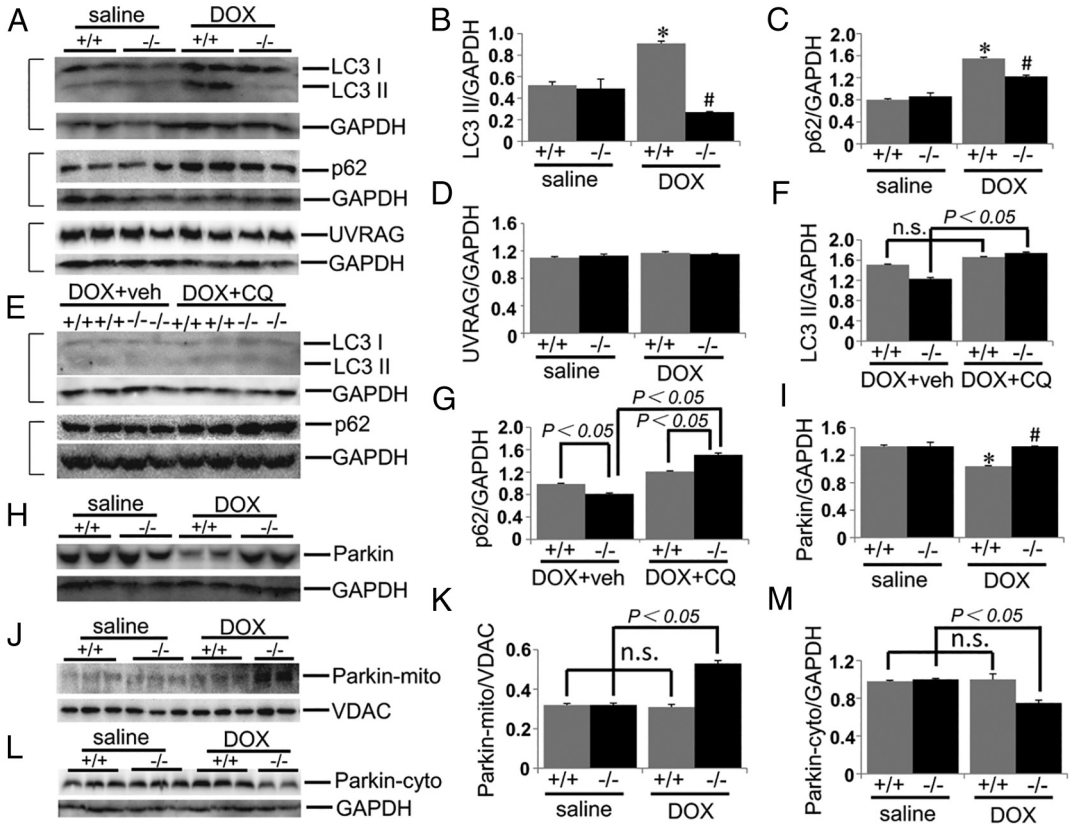

Fig. 3. Loss of Rubicon attenuates DOX-induced impairment of mitophagy in the hearts. (A) Representative images of Western blot of LC3 II, p62 and UVRAG protein levels in the hearts from mice 3 days after DOX or saline treatment. (B) Quantification of LC3 II as illustrated in (A) (n = 4). (C) Quantification of p62 as illustrated in (A) (n = 4). (D) Quantification of UVRAG as illustrated in (A) (n = 4). (E) Western blot of LC3 II and p62 in the hearts from mice 3 days after DOX treatment and further elicited by CQ treatment. (F) Quantification of LC3 II as illustrated in (E) (n = 3). (G) Quantification of p62 as illustrated in (E) (n = 3). (H) Western blot of Parkin protein levels in the hearts from mice 3 days after DOX or saline treatment. (I) Quantification of Parkin as illustrated in (H) (n = 4). (J) Western blot of Parkin protein in mitochondrial fraction from the heart of mice 3 days after DOX or saline treatment. (K) Quantification of mitochondrial Parkin protein levels as illustrated in (J) (n = 4). Parkin-mito: Parkin protein abundance in mitochondrial fraction. (L) Western blot of Parkin protein in cytoplasmic fraction from the hearts of mice 3 days after DOX or saline treatment. (M) Quantification of cytoplasmic Parkin protein levels as illustrated in (L) (n = 4). Parkin-mito, Parkin protein in mitochondrial fraction. Parkin-cyto, Parkin protein in cytoplasmic fraction. $^{*}P < 0.05$ vs. saline+/+, $^{\#}P < 0.05$ vs. DOX+/+.

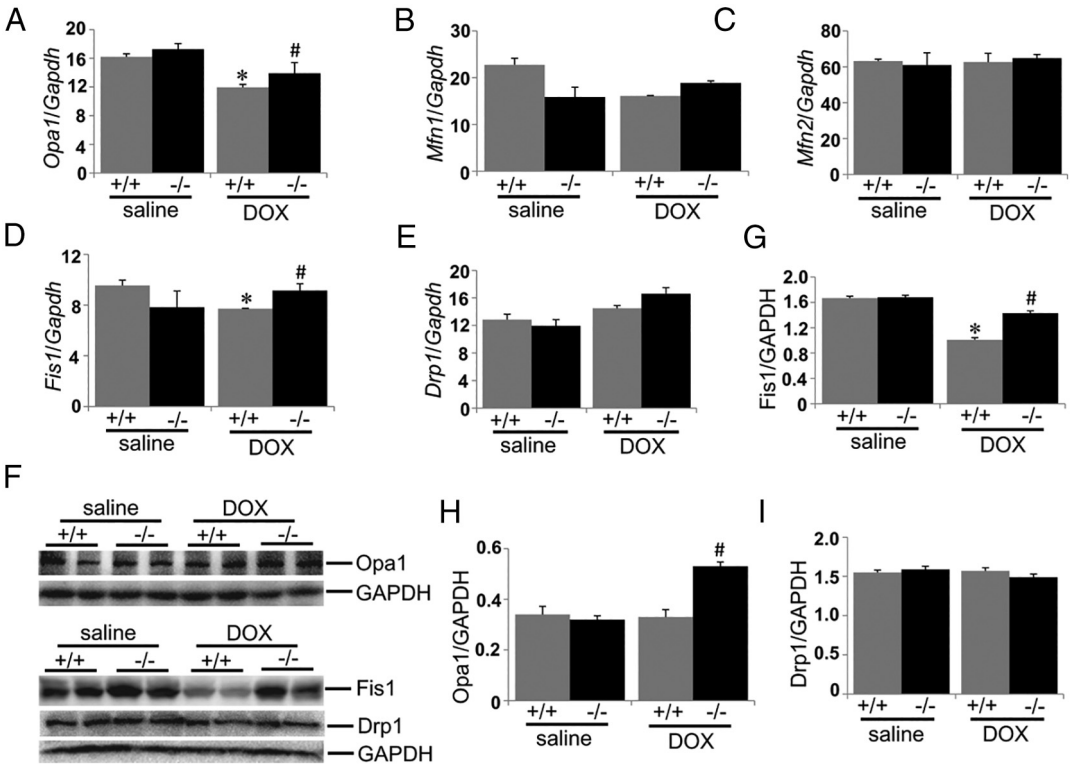

Fig. 4. Impact of Rubicon deficiency on markers of mitochondrial dynamics. Real time RT-PCR analysis of *Opa1* (A), *Mfn1* (B), *Mfn2* (C), *Fis1* (D) and *Drp1* (E) expression in the hearts from mice 3 days after DOX or saline treatment (n = 3). (F) Representative images of Western blot of Opa1, Fis1 and Drp1 expression in the hearts from mice 3 days after DOX or saline treatment. Quantification of Fis1 (G), Opa1 (H) and Drp1 (I) as illustrated in (F) (n = 3). $^{*}P < 0.05$ vs. saline+/+, $^{\#}P < 0.05$ vs. DOX+/+.

We observed a significant reduction in Rubicon expression 16 h, but not 3 and 5 days after DOX treatment. Given that DOX impaired autophagic flux in the heart and induced cardiac damage, which was attenuated by Rubicon deficiency, the early decrease in Rubicon expression may represent a protective response to DOX treatment. Autophagy impairment by DOX could be a critical step for DOX cardiotoxicity as impaired autophagy attenuates clearance of damaged mitochondria and establishes the vicious cycle of ROS-induced ROS release. Previously we and others have shown that DOX disrupts multiple steps of autophagy in the heart including autophagosome formation, maturation and degradation [22–25]. In addition, DOX suppresses Parkin expression and its translocation from cytoplasm to mitochondria (Fig. 3H–M), which impaired mitophagy. Autophagic flux and mitophagy were maintained in Rubicon-deficient mice after DOX treatment, suggesting that loss of Rubicon improves autophagy and mitophagy steps impaired by DOX. Therefore, Rubicon is an ideal target for prevention or therapy of DOX cardiotoxicity.

Loss of Rubicon attenuated mortality of both male and female mice after DOX treatment. However, the survival improvement in Rubicon-deficient mice could not be completely attributed to amelioration of myocardial injury since DOX causes damage to several other vital organs such as liver and kidney [33]. A single intraperitoneal injection of DOX at 20 mg/kg predisposes mice to acute cardiotoxicity, leading to sudden death even before pronounced cardiac remodeling and cardiac dysfunction are present. To test the clinical relevance of Rubicon-deficient mice, we evaluated cardiac morphometry and function by echocardiography in a chronic mouse model of DOX cardiotoxicity. We observed reduced LVPW thickness in DOX-treated WT mice. This observation is consistent with the findings in DOX-treated patients [34]. Importantly, loss of Rubicon attenuated the reduction in LVPW thickness. Cardiac dysfunction was not detected in DOX-treated animals. DOX induces cardiotoxicity in a dose- and time-dependent manner. It is possible that the total cumulative dose of DOX or the dosing time was not sufficient to induce cardiac dysfunction at the time point we performed echocardiography. Time course and dose-dependent analysis of the impact of Rubicon deficiency on cardiac function needs to be assessed in the future.

Mitochondrial Parkin protein was more abundant in the hearts from Rubicon-deficient mice compared with WT controls after DOX treatment, which can be attributed to (i) less Parkin is available for mitochondrial translocation in WT mice due to suppressed Parkin expression caused by DOX. Loss of Rubicon alleviates the suppression of Parkin expression, although the mechanisms remain to be determined. (ii) DOX promotes interaction between p53 and Parkin in the cytoplasm, which prevents Parkin translocation to mitochondria [35]. Loss of Rubicon may disrupt the interaction of cytoplasmic p53 and Parkin.

In DOX-treated WT mice, mitophagy in the heart was blocked, leading to accumulation of damaged mitochondria. However, VDAC protein abundance was not significantly changed in the heart. This may be due to impaired mitochondrial biogenesis, which also contributes to cardiac disease [36]. Indeed, Nrf-1, a key transcription factor regulating mitochondrial biogenesis [37] was significantly reduced in the hearts from DOX-treated WT animals, while loss of Rubicon retained Nrf-1 protein abundance (data not shown). Therefore, mitophagy and mitochondrial biogenesis were both likely impaired by DOX and the impairment was improved by Rubicon deficiency. In addition, our data indicate that mitochondria are less dynamic in the heart after DOX treatment as evidenced by reduced expression of mitochondrial fusion protein Opa1 and fission protein Fis1. Loss of Rubicon likely enables mitochondria to retain relatively higher fission and fusion activities after DOX treatment.

In conclusion, loss of Rubicon ameliorates DOX cardiotoxicity through enhancement of mitochondrial quality by preserving autophagy, mitophagy and remodeling of mitochondrial fission/fusion dynamics in the heart. Rubicon is a potential molecular target for prevention and therapy of DOX cardiotoxicity.

Declaration of Competing Interest

The authors declare that they have no conflicts of interest.

Acknowledgements

This work was supported by research grant from Natural Science Foundation of Shanghai (16ZR1418200); National Natural Science Foundation of China (81974020). We acknowledge Institute of Developmental Biology and Molecular Medicine of Fudan University for providing Rubicon-deficient mice generated by piggyBac transposition.

Appendix A. Supplementary data

Supplementary data to this article can be found online at https://doi.org/10.1016/j.ijcard.2019.07.074.

References

[1] G. Takemura, H. Fujiwara, Doxorubicin-induced cardiomyopathy from the cardiotoxic mechanisms to management, Prog. Cardiovasc. Dis. 49 (2007) 330–352.
[2] Y. Octavia, C.G. Tocchetti, K.L. Gabrielson, et al., Doxorubicin-induced cardiomyopathy: from molecular mechanisms to therapeutic strategies, J. Mol. Cell. Cardiol. 52 (2012) 1213–1225.
[3] M. Schieber, N.S. Chandel, ROS function in redox signaling and oxidative stress, Curr. Biol. 24 (2014) R453–R462.
[4] J.M. Berthiaume, K.B. Wallace, Adriamycin-induced oxidative mitochondrial cardiotoxicity, Cell Biol. Toxicol. 23 (2007) 15–25.
[5] H.M. Ni, J.A. Williams, W.X. Ding, Mitochondrial dynamics and mitochondrial quality control, Redox Biol. 4 (2015) 6–13.
[6] A. Kelekar, Autophagy, Ann. N. Y. Acad. Sci. 1066 (2005) 259–271.
[7] Y. Ikeda, A. Shirakabe, C. Brady, et al., Molecular mechanisms mediating mitochondrial dynamics and mitophagy and their functional roles in the cardiovascular system, J. Mol. Cell. Cardiol. 78 (2015) 116–122.
[8] C. Vives-Bauza, C. Zhou, Y. Huang, et al., PINK1-dependent recruitment of Parkin to mitochondria in mitophagy, Proc. Natl. Acad. Sci. U. S. A. 107 (2010) 378–383.
[9] M. Lazarou, D.A. Sliter, L.A. Kane, et al., The ubiquitin kinase PINK1 recruits autophagy receptors to induce mitophagy, Nature 524 (2015) 309–314.
[10] Y. Chen, G.W. Dorn 2nd, PINK1-phosphorylated mitofusin 2 is a Parkin receptor for culling damaged mitochondria, Science 340 (2013) 471–475.
[11] A. Tanaka, Parkin-mediated selective mitochondrial autophagy, mitophagy: Parkin purges damaged organelles from the vital mitochondrial network, FEBS Lett. 584 (2010) 1386–1392.
[12] D.A. Kubli, X. Zhang, Y. Lee, et al., Parkin protein deficiency exacerbates cardiac injury and reduces survival following myocardial infarction, J. Biol. Chem. 288 (2013) 915–926.
[13] P. Bhandari, M. Song, Y. Chen, et al., Mitochondrial contagion induced by Parkin deficiency in Drosophila hearts and its containment by suppressing mitofusin, Circ. Res. 114 (2014) 257–265.
[14] V. Jazbutyte, Mitochondrial dynamics: molecular mechanisms and the role in the heart, Minerva Cardioangiol. 58 (2010) 231–239.
[15] S.B. Ong, A.R. Hall, D.J. Hausenloy, Mitochondrial dynamics in cardiovascular health and disease, Antioxid. Redox Signal. 19 (2013) 400–414.
[16] J. Marín-García, A.T. Akhmedov, Mitochondrial dynamics and cell death in heart failure, Heart Fail. Rev. 21 (2016) 123–136.
[17] W.W. Sharp, S.L. Archer, Mitochondrial dynamics in cardiovascular disease: fission and fusion foretell form and function, J. Mol. Med. (Berl.) 93 (2015) 225–228.
[18] C. Liang, J.S. Lee, K.S. Inn, et al., Beclin1-binding UVRAG targets the class C Vps complex to coordinate autophagosome maturation and endocytic trafficking, Nat. Cell Biol. 10 (2008) 776–787.
[19] Y.M. Kim, C.H. Jung, M. Seo, et al., mTORC1 phosphorylates UVRAG to negatively regulate autophagosome and endosome maturation, Mol. Cell 57 (2015) 207–218.
[20] Q. Sun, J. Zhang, W. Fan, et al., The RUN domain of rubicon is important for hVps34 binding, lipid kinase inhibition, and autophagy suppression, J. Biol. Chem. 286 (2011) 185–191.
[21] K. Matsunaga, T. Saitoh, K. Tabata, et al., Two Beclin 1-binding proteins, Atg14L and Rubicon, reciprocally regulate autophagy at different stages, Nat. Cell Biol. 11 (2009) 385–396.
[22] L. An, X.W. Hu, S. Zhang, et al., UVRAG deficiency exacerbates doxorubicin-induced cardiotoxicity, Sci. Rep. 7 (2017), 43251.
[23] X. Xu, R. Bucala, J. Ren, Macrophage migration inhibitory factor deficiency augments doxorubicin-induced cardiomyopathy, J. Am. Heart Assoc. 2 (2013), e000439.
[24] T. Kawaguchi, G. Takemura, H. Kanamori, et al., Prior starvation mitigates acute doxorubicin cardiotoxicity through restoration of autophagy in affected cardiomyocytes, Cardiovasc. Res. 96 (2012) 456–465.
[25] D.L. Li, Z.V. Wang, G. Ding, et al., Doxorubicin blocks cardiomyocyte autophagic flux by inhibiting lysosome acidification, Circulation 133 (2016) 1668–1687.
[26] S. Ding, X. Wu, G. Li, et al., Efficient transposition of the piggyBac (PB) transposon in mammalian cells and mice, Cell 122 (2005) 473–483.
[27] Z. Zi, Z. Song, S. Zhang, et al., Rubicon deficiency enhances cardiac autophagy and protects mice from lipopolysaccharide-induced lethality and reduction in stroke volume, J. Cardiovasc. Pharmacol. 65 (2015) 252–261.
[28] L.M. Yu, W.C. Di, X. Dong, et al., Melatonin protects diabetic heart against ischemia-reperfusion injury, role of membrane receptor-dependent cGMP-PKG activation, Biochim. Biophys. Acta Mol. basis Dis. 1864 (2018) 563–578.
[29] C. Gu, T. Li, S. Jiang, et al., AMP-activated protein kinase sparks the fire of cardioprotection against myocardial ischemia and cardiac ageing, Ageing Res. Rev. 47 (2018) 168–175.
[30] Z. Wang, W. Hu, C. Lu, et al., Targeting NLRP3 (nucleotide-binding domain, leucine-rich-containing family, pyrin domain-containing-3) inflammasome in cardiovascular disorders, Arterioscler. Thromb. Vasc. Biol. 38 (2018) 2765–2779.
[31] M. Picard, B.S. McEwen, E.S. Epel, et al., An energetic view of stress: focus on mitochondria, Front. Neuroendocrinol. 49 (2018) 72–85.
[32] D.J. Klionsky, K. Abdelmohsen, A. Abe, et al., Guidelines for the use and interpretation of assays for monitoring autophagy (3rd edition), Autophagy 12 (2016) 1–222.
[33] P. Shivakumar, M.U. Rani, A.G. Reddy, et al., A study on the toxic effects of Doxorubicin on the histology of certain organs, Toxicol. Int. 19 (2012) 241–244.
[34] M. Rathe, N.L. Carlsen, H. Oxhøj, Late cardiac effects of anthracycline containing therapy for childhood acute lymphoblastic leukemia, Pediatr. Blood Cancer 48 (2007) 663–667.
[35] A. Hoshino, Y. Mita, Y. Okawa, et al., Cytosolic p53 inhibits Parkin-mediated mitophagy and promotes mitochondrial dysfunction in the mouse heart, Nat. Commun. 4 (2013) 2308.
[36] J. Ly, C. Deng, S. Jiang, et al., Blossoming 20: the energetic regulator's birthday unveils its versatility in cardiac diseases, Theranostics 9 (2019) 466–476.
[37] R.C. Scarpulla, Nuclear activators and coactivators in mammalian mitochondrial biogenesis, Biochim. Biophys. Acta 1576 (2002) 1–14.